J. Chem. Sci. Vol. 124, No. 6, November 2012, pp. 1315–1325.

Fabrication of optochemical and electrochemical sensors using thin films of porphyrin and phthalocyanine derivatives

PALANISAMY KALIMUTHU, ARUMUGAM SIVANESAN and S ABRAHAM JOHN*
Centre for Nanoscience and Nanotechnology, Department of Chemistry, Gandhigram Rural Institute, Gandhigram, Dindigul 634 302, India
e-mail: abrajohn@yahoo.co.in

Abstract. This paper describes the fabrication of thin films of porphyrin and metallophthalocyanine derivatives on different substrates for the optochemical detection of HCl gas and electrochemical determination of L-cysteine (CySH). Solid state gas sensor for HCl gas was fabricated by coating *meso*-substituted porphyrin derivatives on glass slide and examined optochemical sensing of HCl gas. The concentration of gaseous HCl was monitored from the changes in the absorbance of Soret band. Among the different porphyrin derivatives, *meso*-tetramesitylporphyrin (MTMP) coated film showed excellent sensitivity towards HCl and achieved a detection limit of 0.03 ppm HCl. Further, we have studied the self-assembly of 1,8,15,22-tetraaminometallophthalocyanine (4α-MTAPc; M = Co and Ni) from DMF on GC electrode. The CVs for the self-assembled monolayers (SAMs) of 4α-Co^{II}TAPc and 4α-Ni^{II}TAPc show two pairs of well-defined redox couple corresponding to metal and ring. Using the 4α-Co^{II}TAPc SAM modified electrode, sensitive and selective detection of L-cysteine was demonstrated. Further, the SAM modified electrode also successfully separates the oxidation potentials of AA and CySH with a peak separation of 320 mV.

Keywords. *Meso*-substituted porphyrin; optochemical sensing; HCl gas; 1,8,15,22-tetraaminometallophthalocyanine; L-cysteine.

1. Introduction

Porphyrin and its derivatives are very stable in nature and have strong absorption characteristics in the region of 350 to 750 nm.[1,2] The appearance of strong Soret and Q bands of porphyrins in the visible region encourage the researchers to design these dyes for the fabrication of optochemical sensors. Considering the well-understood ability of heme to bind gases like NO, CO_2, and O_2, porphyrins would indeed seem a suitable choice for the detection of gaseous species.[3] Research in this area has focused on incorporation of synthetic porphyrins and metalloporphyrins into different matrixes including polymers, glasses, and Langmuir–Blodgett (LB) films.[4–11] Since porphyrin derivatives are very stable both thermally and chemically, they have attracted much interest as potential materials for integration into optochemical gas sensors. Hydrogen chloride (HCl) gas is the source for acid rain as well as a work place hazard with a short term exposure limit of 5 ppm and therefore sensing and standardization of its level in the atmosphere are very important. The concentration of HCl in the environment is now strictly regulated in many countries owing to its hazardous nature. Porphyrin, when deposited as a thin film, interacts with inorganic gases such as H_2S, HCl, Cl_2, and NH_3 by absorption on to the sensing layer.[3] The previously reported sensors are mainly based on the incorporation of porphyrin into hydrophobic membrane, ethyl cellulose, sol–gel and polymer composite materials.[4–11] Although many reports were available in the literature for the optochemical detection of HCl gas, fabrication of a solid state sensor for HCl gas with high stability, sensitivity and selectivity is still one of the challenging tasks for the researchers. In this paper, we have employed a very simple procedure to fabricate a solid state sensor by coating the porphyrin derivatives on glass slide and examined optochemical sensing of HCl gas. We have synthesized *meso*-tetramesitylporphyrin (MTMP), *meso*-tetraphenylporphyrin (MTPP) and *meso*-tetrakis-(4-nitrophenyl)porphyrin (MTNP) (scheme 1) and studied their HCl gas sensing properties after coated on glass slides.

Phthalocyanines (Pcs) are macrocyclic 18-π electron aromatic compounds with four isoindoline units joined by four azo nitrogens. This structure is very similar to the naturally occurring porphyrins. Thus, it is interesting to fabricate thin films of both porphyrin and phthalocyanine on solid substrates and examine their optical and electrochemical properties. Replacement of four methine groups in the *meso* position of porphyrin by four azo nitrogens make Pcs more stable towards heat

*For correspondence

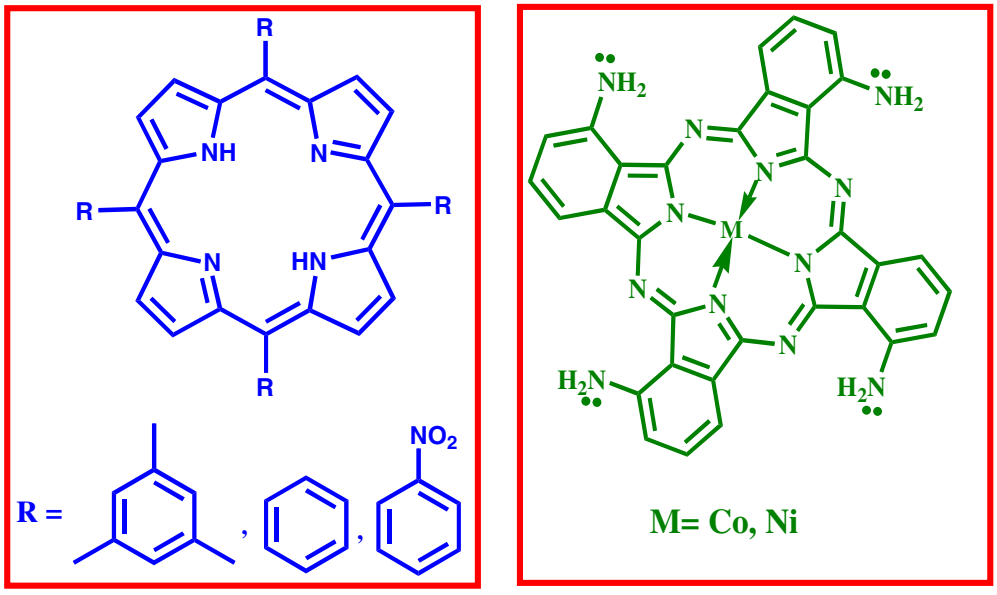

Scheme 1. Structures of (**a**) porphyrin derivatives and (**b**) 1,8,15,22-tetraaminometallophthalocyanine.

and light.[12] Further, substitution of the porphyrin ring with four benzene rings gives greater delocalization of π electron density in Pcs. As a result of this extended delocalization, the electronic spectrum of Pcs show a bathochromic shift in the absorption maximum (λ_{max}) relative to that of porphyrins.[13] The Pcs have greater structural flexibility and hence internal hydrogens in the Pc inner core can be replaced by most of the metals in the periodic table to yield metallophthalocyanines (MPcs). The high thermal and chemical stabilities of MPcs lead to the technological applications in the fields of chemical sensors,[14,15] liquid crystals,[16,17] field effect transistors,[18] electrochromic devices,[19,20] optical data storage systems[21,22] and photodynamic therapy.[23,24] Fabrication of thin films of MPcs on solid substrates has been received great interest to the researchers because of their extensive applications in photovoltaic cells, molecular electronics, optical data storage systems, electrochemical and optochemical sensors and electrochromic devices. Since most of the applications of Pcs were mainly based on thin films formed on solid substrates it is very important to find a suitable method to prepare an ordered film on solid substrates with high stability. Various methods have been used for the fabrication of MPc thin films which include direct deposition of MPc solution on electrode surface via casting,[25] electropolymerization,[26] self-assembly (SA),[27] spin coating[28] and vapour deposition.[29] Among these methods, modification of electrode surface by SA method using MPcs is one of the elegant methods because highly ordered films can be prepared easily on the electrode surface by this method. Further, thin films of MPcs prepared by this method yields reproducible results and much stable for long term usage.[30] The self-assembled monolayer (SAM) of Pcs on different substrates was achieved by tethering the Pc with carboxylic acid, trichlorosilyl, and thiol or thioether groups. One of the important issues for these Pcs is the tedious procedure involved in the synthesis and also ends up with low yield. Further, the organosulphur functionalized Pcs are unstable in atmospheric conditions. Recently, it has been shown that Pcs tethered with amine functional groups can also form SAM on Ag and Au substrates. However, Au and Ag electrodes used for the SAM formation have limited potential window for electrocatalytic applications. Thus, in the present study, we have investigated the self-assembly of amine functionalized MPcs (1,8,15,22-tetraaminometallophthalocyanine (4α-MTAPc; M = Co, Ni; scheme 1) on glassy carbon (GC) electrode. Further, the SAM of 4α-Co^{II}TAPc was successfully used for the determination of L-cysteine.

2. Experimental

2.1 *Chemicals*

L-cysteine (CySH) and ascorbic acid (AA) were purchased from Aldrich and were used as received. All other chemicals used in this investigation were of analytical grade and were used as received. Deionized water was prepared by double distillation with alkaline

$KMnO_4$. Acetate buffer solution was prepared using sodium acetate and acetic acid. *meso*-tetramesitylporphyrin (MTMP), *meso*-tetraphenylporphyrin (MTPP) and *meso*-tetrakis-(4-nitrophenyl)porphyrin (MTNP) MTMP were synthesized according to the reported procedure.[31]

2.2 *Fabrication of solid state sensor*

The solid state sensor for HCl gas detection was fabricated by depositing a thin film of a porphyrin on cleaned glass slide (0.8 mm × 300 mm) using dip coating method. Clean glass slide was immersed in the 0.01 mM MTMP dissolved in chloroform at the rate of 12 cm/min and dried at room temperature under nitrogen atmosphere. A home-made pulsed generator with a stepper at a withdrawal speed of 12 cm/min was used to deposit a thin film of porphyrin on glass slide. The same procedure was followed for sensor fabrication using MTPP and MTNP. The porphyrin deposited glass slide was dried at room temperature under nitrogen atmosphere for 10 min. Standard dry HCl gas (19 ppm) diluted with nitrogen was used and the concentration of HCl gas was controlled by mixing the standard gas with nitrogen. Mass flow controller was used to mix the desired amount of HCl gas with dry nitrogen. All measurements were performed at room temperature.

2.3 *Self-assembly of 4α-MTAPc on GC surface*

1,8,15,22-Tetraaminophthalocyanatocobalt(II) and Ni(II) were synthesized based on the reported procedure.[32] The SAM of 4α-MTAPc was formed by soaking the cleaned GC electrode in completely deaerated dimethylformamide (DMF) containing 1 mM 4α-MTAPc at different time intervals. The electrode was then removed from the solution and repeatedly washed with DMF. The charge under the anodic wave corresponding to Co(II) oxidation was used to calculate the surface coverage without subtracting the electrode roughness factor.

2.4 *Instrumentation*

Perkin Elmer Lambda 35 spectrophotometer was used to record the UV-vis absorption spectra. Electrochemical measurements were performed in a conventional two compartment three electrode cell with a mirror polished glassy carbon (GC) as a working electrode. Pt wire as counter electrode and KCl saturated Ag/AgCl as reference electrode. The electrochemical measurements were carried out with CHI model 643B (Austin, TX, USA) Electrochemical Workstation. Raman spectra were recorded using a Renishaw Raman microscope, with the 514 nm Ar+ ion laser for excitation. All the electrochemical measurements were carried out under nitrogen atmosphere at room temperature. AFM images were obtained using MultiMode V scanning Probe Microscope for MTMP coated glass plates.

3. Results and discussion

3.1 *Characterization of the solid state sensor*

The UV-vis spectrum obtained for MTMP deposited glass slide shows a more intense absorbance for Soret band at 438 nm along with less intense peaks at 521, 549, 595, and 650 nm corresponding to Q bands (figure 1 (curve a)). The observed characteristic spectral bands of MTMP deposited glass slide clearly indicate that MTMP was adsorbed on the glass slide. In contrast to MTMP in dichloromethane (figure S1; supporting information), a 16 nm red shift in the Soret band was observed for MTMP deposited glass slide. This may be attributed to the aggregation of the porphyrin molecules in solid state.[33] When the MTMP deposited glass slide was exposed to HCl vapour, not only the Soret band was shifted from 438 to 453 nm but also intensities were found to increase at 453 and 650 nm (curve b). The observed 15 nm shift in the Soret band with an increase in intensities at both 453 and 650 nm was attributed to the formation of J-aggregates. Further, the aggregation of MTMP molecules upon protonation was confirmed

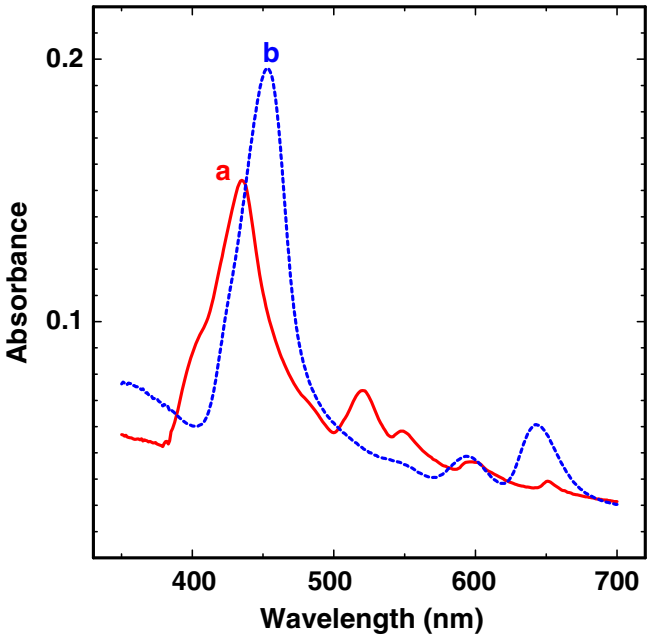

Figure 1. Absorption spectra obtained for MTMP film coated on glass slide (a) before and (b) after exposed to HCl vapour.

by AFM studies. Figure 2a shows the tapping mode 2-D AFM image of the glass slide coated with MTMP. The thickness of the thin film was found to be 10 nm (figure 2b). When this film was exposed to HCl vapour for a minute, aggregated structure was obtained (figure 2c). The 3D view (figure 2d) indicated that the nanostructures of MTMP aggregates were grown vertically in contrast to MTMP thin film. Rearranged Beer–Lambert equation was used to calculate the surface density (d_{surf}) of the porphyrin molecules.[34]

$$d_{surf} = A \times \varepsilon^{-1} \quad (1)$$

where A is the Soret band absorbance of MTMP and ε is molar extinction coefficient. The surface density of MTMP molecules in MTMP film was found to be 6.7×10^{-7} mol cm^{-2}.

3.2 *Detection of HCl gas*

To obtain quantitative information about the sensing properties of solid state sensor, UV-vis spectra were recorded and the corresponding responses for successive exposure of HCl vapour to solid state sensor are shown in figure 3. As the exposure time of HCl increases, the absorbance of Soret band at 452 nm increases significantly in addition to other bands. The absorbance changes of Soret band at 452 nm were monitored with respect to the concentration of exposed HCl gas. As shown in figure 3, the solid state sensor shows a sharp increase in the absorbance after exposed to 0.4 ppm HCl gas which implies the sensing capability of solid state sensor towards HCl gas.

Exposure of the sensor to HCl gas leads to the conversion of MTMP into PMTMP and thus the intensity of Soret band at 452 nm sharply increases (figure 4). When an inert gas (N_2) was passed after reaching the equilibrium state, the Soret band intensity at 452 nm started to decrease and attained the original intensity as observed for MTMP suggesting that PMTMP was reverted to MTMP. A set of four successive HCl exposures to solid state sensor was carried out in the range of 0.4–0.1 ppm (figure 4). The sensor showed good response to even at the concentration of 0.1 ppm HCl gas with good

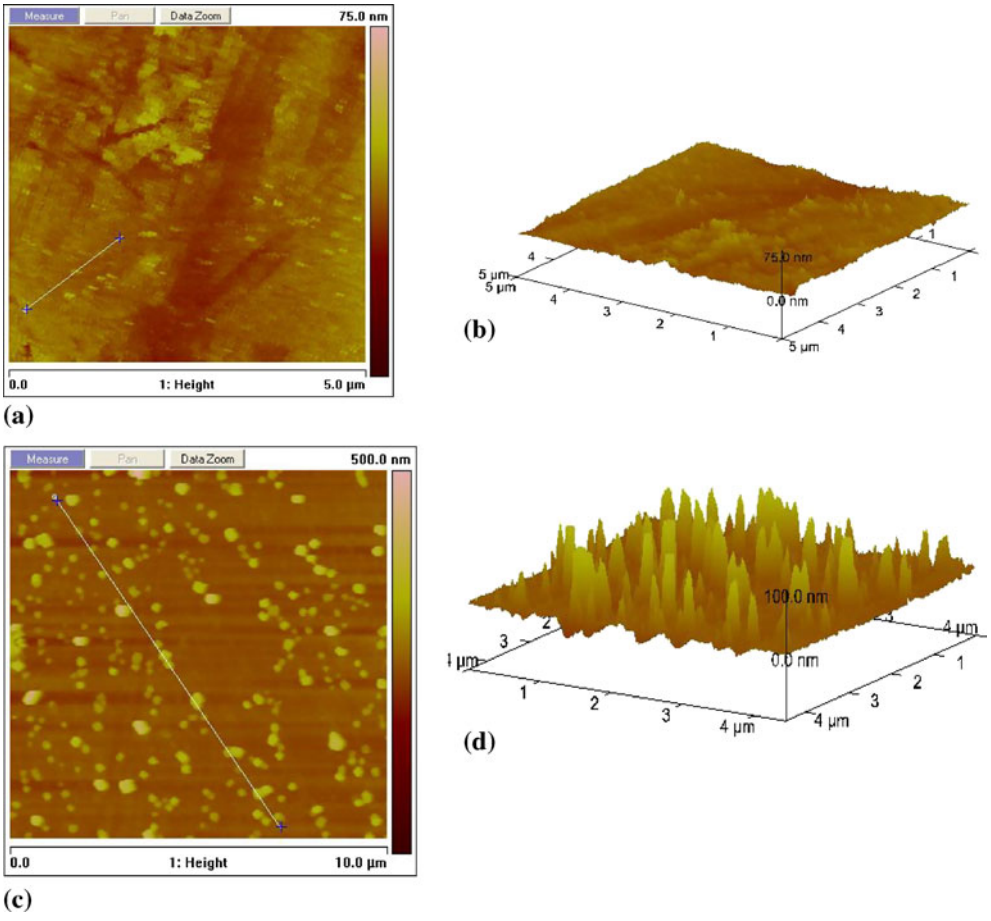

Figure 2. Tapping mode AFM images of the glass slide coated with MTMP before (**a**) 2D and (**b**) 3D views and (**c**) 2D and (**d**) 3D views after exposed to HCl vapour.

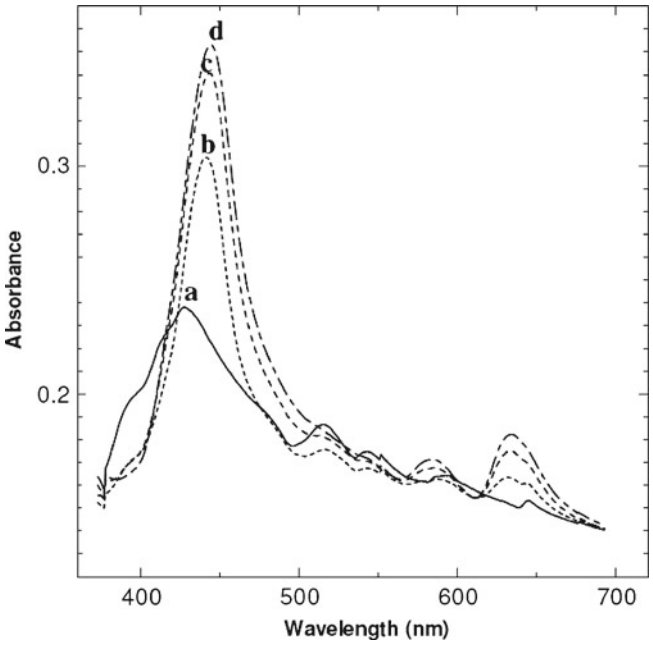

Figure 3. Absorption spectra of MTMP deposited glass plate before (a) and after (b) 5, (c) 120, and (d) 180 s exposure to 0.4 ppm HCl vapour.

reversibility. Absorbance variation (ΔA) was obtained from the differences between the absorbance intensities of the MTMP thin film at 452 nm before and after exposure to different HCl concentrations.[35] To obtain the calibration curve, we have plotted the concentrations of HCl against the (ΔA). As the concentration of HCl gas increases, the absorbance of the Soret band also increases yielding the following equation

$$\begin{aligned} Absorbance \;=\; & 0.1692\,(\pm 0.0118) \\ & \times concentration \\ & + 0.06135\,(\pm 0.0032) \end{aligned} \qquad (2)$$

(Number of data = 4 ; correlation coefficient = 0.9959). The complete reversibility of 0.4 ppm HCl gas exposed sensor was attained after passing N_2 for 16 min, which indicates that the sensor is fully reversible but the rate of reversal is markedly slower than the rate of the response. The detection limit of the solid state sensor found to be 0.03 ppm. The detection limit was measured by analysing standards that are zero in concentration then measuring the standard deviation of the measurements. In order to reduce the probability of a false non-detection, the standard deviation is then multiplied by the factor 3.0.[36]

3.3 *Optochemical sensing of HCl gas using MTPP deposited glass slide*

The HCl sensing properties of MTPP film was studied similar to MTMP. The MTPP was coated on a glass slide and used for HCl sensing. The protonation of MTPP (figure 5) leads to 15 nm red shift of Soret band. The deprotonation of the porphyrin was checked with flushing of N_2 gas and found that the reversibility of

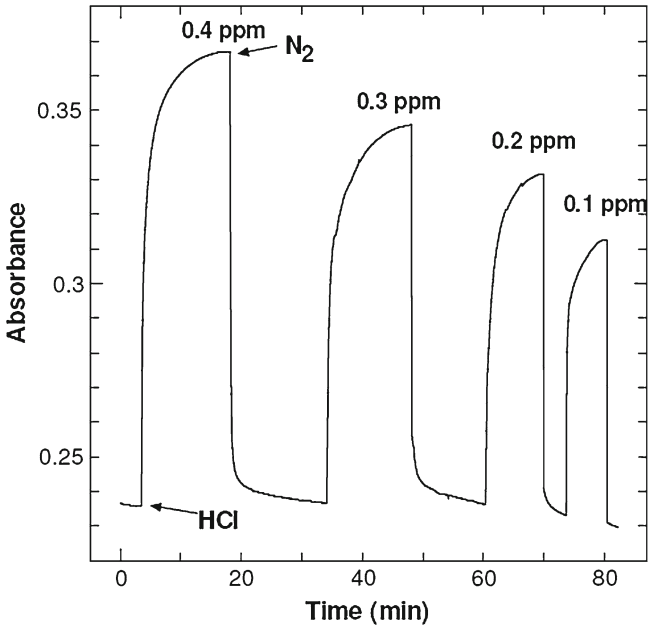

Figure 4. Absorption response and recovery of MTMP deposited glass plate for successive exposures to HCl gas in the range of 0.4-0.1 ppm.

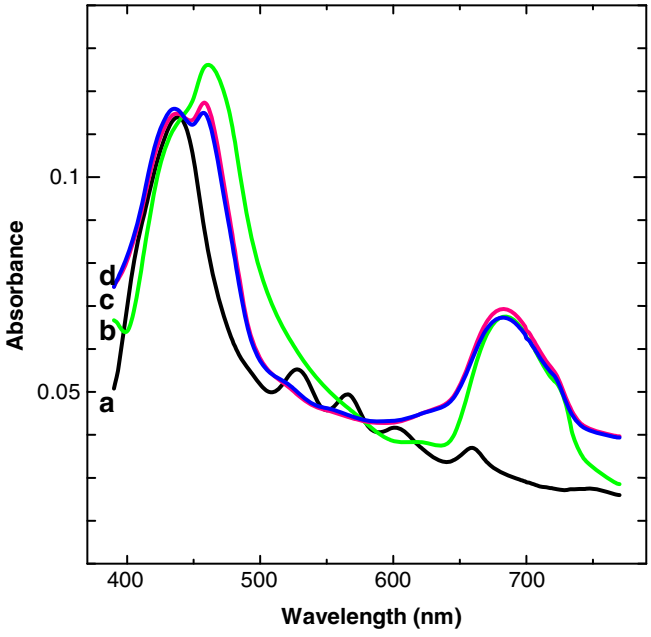

Figure 5. Absorption spectra of MTPP deposited glass plate (a) before and (b) after 180 s exposure to 0.4 ppm HCl vapour. The same film after flushing with nitrogen gas for (c) 1200 and (d) 3200 s.

MTPP is very poor (figure 5). The reversibility was not observed even after 1 h of flushing out with N_2 gas (figure 6a). The absorption changes of MTPP coated glass slide towards the HCl gas is shown in figure 6a. After the introduction of HCl gas, the absorption at 458 nm sharply increased. After reaching the steady state, the HCl gas was cut off and the N_2 flush out was introduced. The decrease in absorption was not sharp and regular. The complete reversibility was not achieved even after 45 min. This indicated that the MTPP coated film can not be used as HCl sensor. The poor reversibility of the sensor may be due to the absence of bulky group like mesityl at *meso* positions.

3.4 *Optochemical sensing of HCl gas using MTNP deposited glass slide*

Similar to MTPP, MTNP film was also screened for the HCl sensing properties. The MTNP was coated on a glass slide and used for HCl sensing. The protonation of MTNP (figure S2 in the supporting information) leads to 23 nm red shift of Soret band. The protonation of MTNP by HCl gas was not resulted in a significant change in the absorption of the Q band at 670 nm as in the case of MTMP or MTPP (figure S2). The absorption changes of MTNP coated glass slide towards HCl gas is shown in figure 6b. After the introduction of HCl gas, the absorption at 461 nm sharply increased. After reaching the steady state, the HCl gas was cut-off and the N_2 gas flush out was introduced. The decrease in absorption was not sharp and complete reversibility was not observed even after 45 min. The observed results indicated that MTNP coated glass slide can not be used HCl sensing due to the poor reproducibility. The poor reversibility of the MTNP coated glass slide may be due to the flexibility of porphyrin ring in the absence of bulky group like mesityl at *meso* positions in addition to the different organization of the MTNP molecules on the solid surface.

3.5 *Adsorption of 4α-Co^{II}TAPc on GC electrode*

The SA of 4α-Co^{II}TAPc on GC electrode was followed by cyclic voltammetry (CV). CVs obtained for 4α-Co^{II}TAPc adsorbed on GC electrode at different immersion time intervals in DMF containing 1 mM 4α-Co^{II}TAPc at a scan rate of 0.1 V s^{-1} in 0.1 M H_2SO_4 are shown in figure S3. The 4α-Co^{II}TAPc adsorbed on GC electrode for 10 s shows a well-defined two pairs of redox peaks (curve a). The $E_{1/2}$ of 0.36 V with a peak separation of 0.36 V was observed for a redox peak appeared at less positive potential. This redox wave was assigned to Co^{III}/Co^{II} redox couple based on the earlier reports.[32,37,38] On the other hand, the redox peak appeared at more positive potential was assigned to Pc ring based redox couple i.e., $Co^{III}Pc^{1-}/Co^{III}Pc^{2-}$. As the adsorption time of GC electrode in 4α-Co^{II}TAPc solution increased, the charge under the redox peaks were gradually increased while the redox peak potentials were almost unchanged. This indicated that more and more molecules were adsorbed on the GC electrode as the adsorption time was increased. The charge under the redox peaks increased up to 3 h immersion time and after that it remained constant indicating that 4α-Co^{II}TAPc required 3 h time to attain the saturation coverage.

Further, it was noted from the CVs shown in figure S3 that as the immersion time increased, the capacitance current also increased along with Faradaic charge. Generally, the capacitance current of the double-layer

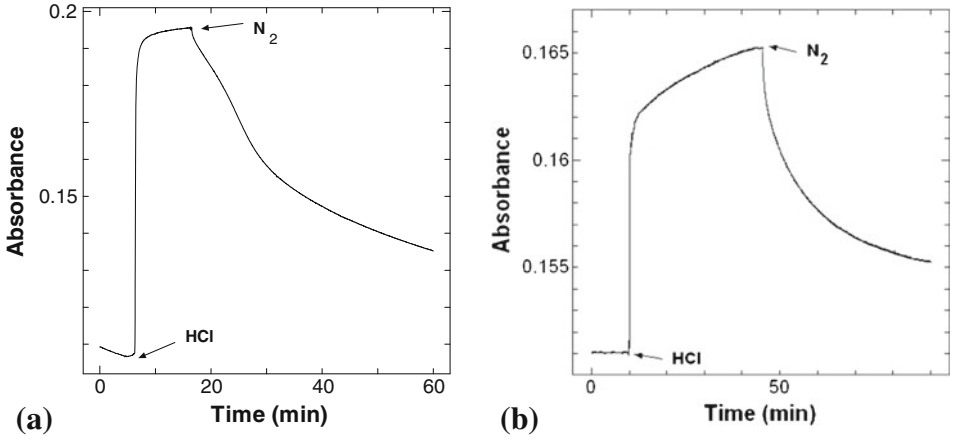

Figure 6. (**a**) Absorption changes at 458 nm of MTPP deposited glass plate exposed to 0.4 ppm HCl vapour. (**b**) Absorption changes at 461 nm of MTNP deposited glass plate exposed to 0.4 ppm HCl vapour.

increases as the dielectric behaviour of terminal group substituted in the SAM increases.[39] Raman spectral studies confirmed that all the four amino groups of 4α-Co^{II}TAPc were not involved in the chemisorption on carbon surface.[32,38] Hence, as the adsorption of 4α-Co^{II}TAPc on GC electrode was increased, the population of free amino groups was also increased which in turn leads to the increase in capacitance current. However, the peak potentials and shape of the CV remained same for several continuous potential cycles demonstrating that the monolayer was highly stable. The surface coverage (Γ) was calculated for 4α-Co^{II}TAPc adsorbed on GC electrode at different time intervals by integrating the charge under the anodic wave corresponding to Co^{II} to Co^{III}. It was found that surface coverage value increased when the adsorption time of 4α-Co^{II}TAPc on GC electrode increased and saturation coverage (Γ_s) of 2.37×10^{-10} mol cm^{-2} was reached after 3 h. Surprisingly, 45% of the surface coverage (1.07×10^{-10} mol cm^{-2}) of 4α-Co^{II}TAPc on GC surface was achieved within 10 s, indicating that the adsorption of 4α-Co^{II}TAPc on GC electrode is very fast. According to previous reports, the CoPc molecule lying flat on the surface with an umbrella configuration will occupy an area close to 200 Å^2 with a surface coverage of approximately 1×10^{-10} mol cm^{-2}.[40,41] However, in the present case, the estimated surface coverage for 4α-Co^{II}TAPc was nearly 2.5 times higher than that of perfectly flat oriented CoPc. There are two possible reasons for the observed higher coverage of 4α-Co^{II}TAPc on GC electrode. One reason is surface roughness of the GC electrode and due to this it is likely that more number of 4α-Co^{II}TAPc molecules was adsorbed on the GC electrode.[42] The second reason is that 4α-Co^{II}TAPc molecules did not adopt perfect flat orientation on GC surface and this was confirmed from Raman spectral studies.[38]

3.6 *Electrochemical behaviour of 4α-Co^{II}TAPc SAM on GC electrode*

Figure 7a shows the CVs of 4α-Co^{II}TAPc SAM on GC electrode in 0.1 M H_2SO_4 at different scan rates for both metal and Pc ring based redox couples. The CVs were consistent in all respects with that expected for an electrochemically reversible reaction involving a surface confined species. For example, the ΔE values were very small (45 mV) and the peak current varied linearly with υ in the range of 0.1–1.0 Vs^{-1} (inset of figure 7a) confirming that the observed redox reaction was due to surface confined species. Further, the CV was stable upon repeated potential cycling. The stability of the SAM of 4α-Co^{II}TAPc on GC electrode was checked by exposing the modified electrodes in the atmospheric air for a month. Even after a month, the electrodes showed the CV similar to that of electrodes not exposed to air (figure not shown). Further, these electrodes were also showed stable CV after 5 min sonication. Such an excellent physical and chemical stability is owing to the strong chemical interaction with the underlying electrodes and not because of simple physical interaction.

Figure 7b shows the CVs obtained for the SAM of 4α-Ni^{II}TAPc on GC electrode in 0.1 M H_2SO_4 at different scan rates. SAM of 4α-Ni^{II}TAPc showed two pairs of well-defined reversible redox peak (curve a). The peak labelled as I has an $E_{1/2}$ and ΔE of 0.37 V and 62 mV, respectively and the peak labelled as II has $E_{1/2}$ and ΔE of 0.63 V and 73 mV, respectively. Based on the earlier reports,[26] the redox wave I was

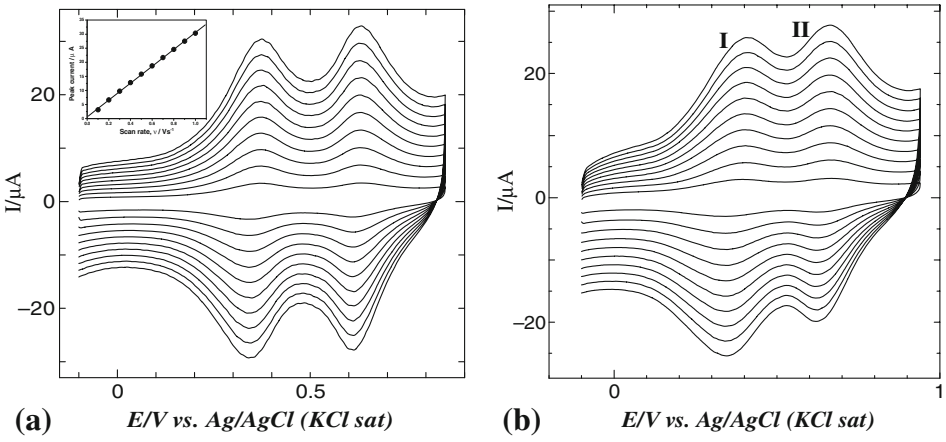

Figure 7. (**a**) CVs of SAM of 4α-Co^{II}TAPc on GC electrode in 0.1 M H_2SO_4 at scan rates of 0.1, 0.2, 0.3, 0.4, 0.5, 0.6, 0.7, 0.8, 0.9 and 1.0 V s^{-1}. (**b**) CVs of self-assembled 4α-Ni^{II}TAPc GC electrode in 0.1 M H_2SO_4 at scan rates of 0.1, 0.2, 0.3, 0.4, 0.5, 0.6, 0.7, 0.8, 0.9 and 1.0 V s^{-1}.

assigned to nickel metal centre redox process specifically Ni^{III}/Ni^{II} and the redox wave II was assigned to $Ni^{III}Pc^{1-}/Ni^{II}Pc^{2-}$. The CVs were consistent in all respects with that anticipated for an electrochemically reversible reaction involving a surface confined species. For example, the ΔE values were typically small and the peak current varied linearly with υ in the range of 0.1–0.8 V s^{-1} confirming that the observed redox reaction was due to surface confined species.

3.7 *Electrochemical behaviour of L-cysteine at 4α-Co^{II}TAPc SAM modified GC electrode*

Before examining the electrocatalytic activity of 4α-Co^{II}TAPc SAM modified GC electrode towards CySH, we have examined the electrochemical behaviour of 4α-Co^{II}TAPc SAM modified electrode in acetate buffer solution. It shows two pairs of well-defined redox peaks for the SAM of 4α-Co^{II}TAPc on GC electrode (figure 8). The redox peak I at less positive potential with an $E_{1/2}$ and ΔE of 0.16 V and 40 mV, respectively due to Co^{III}/Co^{II} redox couple. On the other hand, the redox peak II at higher positive potential with an $E_{1/2}$ and ΔE of 0.40 V and 22 mV, respectively corresponds to $Co^{III}Pc^{-1}/Co^{III}Pc^{-2}$.[32,38] We have examined the electrocatalytic activity of 4α-Co^{II}TAPc SAM modified GC electrode towards CySH oxidation by varying the surface coverage of the SAM and found that the saturated surface coverage of 2.37×10^{-10} mol cm^{-2}, prepared by 3 h adsorption of GC electrode in 4α-Co^{II}TAPc solution showed higher oxidation current for CySH. We have also studied the CySH oxidation by varying the pH and higher current was observed at pH 5.0. Thus, CySH oxidation studies are carried out at pH 5.0 using the 4α-Co^{II}TAPc modified electrode with a saturated surface coverage.

CVs obtained for 0.5 mM CySH at bare GC and 4α-Co^{II}TAPc SAM modified GC electrodes in 0.2 M acetate buffer solution (pH 5.0) are shown in figure 9. At bare GC electrode, a shoulder wave was obtained for the oxidation of CySH around 0.65 V (curve a). Interestingly, the SAM modified electrode exhibited a well-defined oxidation peak at 0.45 V for CySH (curve b). At this electrode, nearly seven-fold higher oxidation current and 200 mV less positive potential shift were observed for CySH when compared to that of bare GC electrode. Now, a doubt may arise whether the observed high current with less positive potential for CySH is due to the mediation of Co^{II} or electrostatic interactions between CySH and free amine groups of 4α-Co^{II}TAPc. In order to clarify this doubt, the electrochemical oxidation of CySH was carried out at the SAM of free base 1,8,15,22-tetraaminophthalocyanine (4α-H_2TAPc) modified GC electrode prepared under identical conditions as used for 4α-Co^{II}TAPc. It is also showed a poor voltammetric response for CySH oxidation like bare GC electrode (curve c). This result clearly confirmed that Co^{II} was mediated the oxidation of CySH.

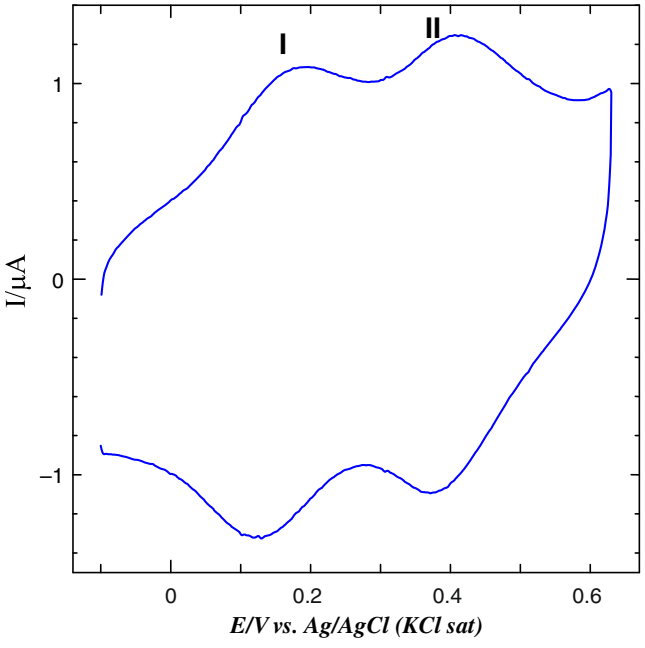

Figure 8. CV obtained for the SAM of 4α-Co^{II}TAPc on GC electrode in 0.2 M acetate buffer solution (pH 5.0) at a scan rate of 0.05 V s^{-1}.

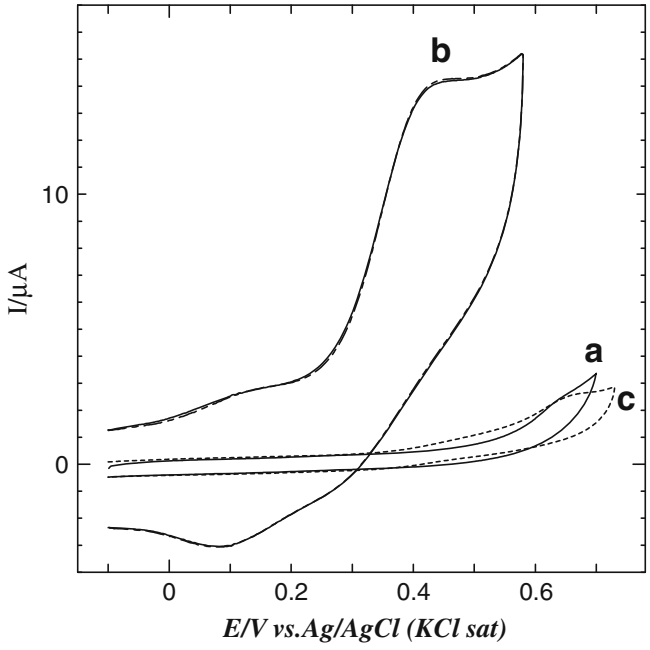

Figure 9. CVs obtained for 0.5 mM CySH at (a) bare GC electrode, (b) 4α-Co^{II}TAPc and (c) 4α-H_2TAPc modified GC electrodes in 0.2 M acetate buffer solution (pH 5.0) at a scan rate of 0.05 V s^{-1}.

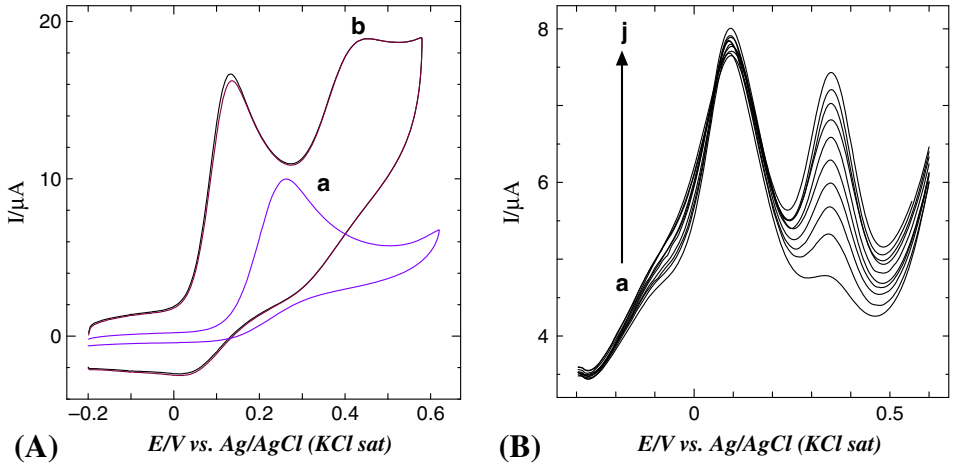

Figure 10. (**A**) CVs obtained for 0.5 mM each AA and CySH at (A) bare and (B) 4α-Co^{II}TAPc SAM modified GC electrodes in 0.2 M acetate buffer solution (pH 5.0) at a scan rate of 0.05 V s^{-1}. (**B**) DPVs obtained for 10 μM CySH containing 200 μM AA at 4α-Co^{II}TAPc SAM modified GC electrode in 0.2 M acetate buffer solution (pH 5.0) (curve a). Each addition increases the concentration of CySH by 10 μM (b–j) keeping the concentration of AA as constant.

Based on the results obtained in the present study and previous reports,[43,44] we are proposing the following mechanism for the oxidation of CySH at 4α-Co^{II}TAPc SAM modified electrode.

$$4\alpha\text{-}Co^{II}TAPc_{(surface)} \rightarrow 4\alpha\text{-}Co^{III}TAPc_{(surface)} + e^{-}$$

$$4\alpha\text{-}Co^{III}TAPc_{(surface)} + CySH_{(aq)} \rightarrow 4\alpha\text{-}Co^{II}TAPc_{(surface)} + CyS^{\cdot}_{(aq)} + H^{+}_{(aq)}$$

$$2CyS^{\cdot}_{(aq)} \rightarrow CySSCy_{(aq)} \text{ (cystine)}.$$

The oxidation of CySH at 4α-Co^{II}TAPc SAM modified electrode was due to two-step process viz., an electrochemical process followed by a chemical reaction. The first step is a one electron electrochemical oxidation of Co^{II} to Co^{III}. The second step is the chemical oxidation of CySH to cysteine radical by Co^{III} species. The generated cysteine radical was highly unstable and instantaneously reacts with another cysteine radical to form a disulphide compound, cystine.

3.8 *Selective determination of CySH in the presence of AA*

AA is one of the major interferences which will encounter in the determination of CySH in biological fluids.[45] Therefore, determination of CySH in the presence of AA is very important for practical applications. Figure 10a shows the CVs obtained for 0.5 mM each of AA and CySH at bare GC and 4α-Co^{II}TAPc SAM modified GC electrodes in 0.2 M acetate buffer solution (pH 5.0). Bare GC electrode showed only one oxidation peak for the mixture of AA and CySH (curve a). Interestingly, 4α-Co^{II}TAPc SAM modified electrode showed well-separated oxidation peaks for AA (0.13 V) and CySH (0.45 V) with a peak separation of 320 mV (curve b) which was more than enough to selectively determine CySH in the presence of AA. The concentration of AA in the biological fluids is usually higher than the concentration of CySH. Therefore, the determination of CySH in the presence of higher concentration of AA is very important in the clinical point of view. Figure 10b shows the DPV obtained for 10 μM of CySH in the presence of 200 μM of AA in 0.2 M acetate buffer solution (pH 5.0) at 4α-Co^{II}TAPc SAM modified GC electrode. It showed a clear signal for CySH oxidation even in the presence of 200 μM of AA. This indicated that the detection of low concentration of CySH is possible in the presence of 20-fold higher concentration of AA. With the addition of 10 μM of CySH to a solution of 200 μM of AA, the oxidation peak current of CySH was linearly increased with a correlation coefficient of 0.9992 while the peak current of AA remained unchanged. These results clearly revealed that 4α-Co^{II}TAPc SAM modified GC electrode is selective towards CySH oxidation in the presence of higher concentration of AA.

4. Concluding remarks

In the first part of the work, we have adopted a very simple procedure to fabricate the solid state sensor by coating *meso*-substituted porphyrin derivatives on glass

slide (solid state sensor) and examined optochemical sensing of HCl gas. Among the different porphyrin derivatives, *meso*-tetramesitylporphyrin (MTMP) coated film showed excellent sensitivity towards HCl. The concentration of gaseous HCl was monitored from the changes in the absorbance of Soret band of PMTMP at 452 nm. The MTMP sensor proposed in this paper has several advantages including ease in preparation and high stability against humid conditions. The lowest detection limit of 0.03 ppm HCl was obtained for the present solid state sensor. On the other hand, the other porphyrin derivatives, MTPP and MTNP coated glass slides were not suitable for HCl gas sensing due to their irreversible nature towards protonation and deprotonation.

In the second part of this paper, we have demonstrated the spontaneous self-assembly of 1,8,15,22-tetraaminometallophthalocyanine on GC electrode. The CVs for the SAMs of 4α-Co^{II}TAPc and 4α-Ni^{II}TAPc show two pairs of well-defined redox couple corresponding to metal and ring. Further, highly sensitive and selective detection of L-cysteine using the 4α-Co^{II}TAPc SAM modified GC electrode was demonstrated. The 4α-Co^{II}TAPc SAM modified electrode mediates the oxidation of CySH not only by enhancing its oxidation current but also shifting its potential towards less positive potential. Further, the SAM modified electrode successfully separates the oxidation potentials of AA and CySH with a peak separation of 320 mV. The fabrication of the present modified electrode was simple and no need to preserve it in buffer solution.

Supporting material

Figures S1–S3 can be seen in www.ias.ac.in/chemsci.

Acknowledgements

We thank the Department of Science and Technology (DST), New Delhi under Nanomission and Defence Research and Development Organization (DRDO), New Delhi for their generous financial support. We thank Mr. A John Jeevagan, Senior Research Scholar for his help.

References

1. Khairutdinov R F and Serpone N 1999 *J. Phys. Chem. B* **103** 761
2. Baraldi I, Carnevali A, Ponterini G and Vanossi D 1995 *J. Mol. Struct. (Theochem)* **333** 121
3. Supriyatno H, Yamashita M, Nakagawa K and Sadaoka Y 2002 *Sens. Actuators B: Chem.* **85** 197
4. Luca G, Pollicino G, Romeo A, Scolaro L M 2006 *Chem. Mater.* **18** 2005
5. Itagaki Y, Deki K, Nakashima S and Sadaoka Y 2006 *Sens. Actuators B: Chem.* **117** 302
6. Nakagawa K, Sadaoka Y, Supriyatno H, Kubo A, Tsutsumi C and Tabuchi K 2001 *Sens. Actuators B: Chem.* **76** 42
7. Nakagawa K, Kumon K, Tsutsumi C, Tabuchi K, Kitagawa T and Sadaoka Y 2000 *Sens. Actuators B: Chem.* **65** 138
8. Supriyatno H, Yamashita M, Nakagawa K and Sadaoka Y 2002 *Sens. Actuators B: Chem.* **85** 197
9. Nakagawa K, Kitagawa T and Sadaoka Y 1998 *Sens. Actuators B: Chem.* **52** 10
10. Nakagawa K, Tanaka K, Kitagawa T and Sadaoka Y 1998 *J. Mater. Chem.* **8** 1199
11. Itagaki Y, Deki K, Nakashima S I and Sadaoka Y 2005 *Sens. Actuators B: Chem.* **1** 393
12. Sobbi A K, Wohrle D and Schlettwein D 1993 *J. Chem. Soc. Perkin Trans. II* 481
13. Stillman M J and Nyokong T 1989 In: *Phthalocyanines: Properties and applications,* Leznoff C C and Lever A B P (eds), New York: VCH Publishers, Vol. **1**
14. Huang J, Virji S, Weiller B H and Kaner R B 2003 *J. Am. Chem. Soc.* **125** 125
15. Adhikari B and Majumdar S 2004 *Prog. Polym. Sci.* **29** 699
16. Collins R A and Mohammed K A 1988 *J. Phys. D: Appl. Phys.* **21** 154
17. Zagal J, Bedioui F and Dodelet J P (eds) 2006 *N4-macrocyclic metal complexes*, New York: Springer
18. Bao Z, Lovinger A J and Dodabalapur A 2006 *Appl. Phys. Lett.* **69** 3066
19. Lin C L, Lee C C and Ho K C 2002 *J. Electroanal. Chem.* **81** 524
20. Somani P R and Radhakrishnan S 2003 *Mater. Chem. Phys.* **77** 117
21. McKeown N B 1998 *Phthalocyanine materials: Synthesis, structure and function*, Cambridge: Cambridge University Press
22. Gu D, Chen Q, Tang X, Gan F, Shen S, Liu K and Xu H 1995 *Opt. Commun.* **121** 125
23. Singerski R, Kalinowski J, Davoli I and Stizza S 1991 *Phys. Status Solidi A* **125** 597
24. Bonnett R 1995 *Chem. Soc. Rev.* **24** 19
25. Wohrle D, Kaune H, Schumann B and Jaeger N 1986 *Macromol. Chem. Phys.* **187** 2947
26. Sivanesan A and John S A 2008 *Electrochim. Acta* **53** 6629
27. Simpson T R E, Cook M J, Petty M C, Thorpe S C and Russell D A 1996 *Analyst* **121** 1501
28. Cook M J 1996 *J. Mater. Chem.* **6** 677
29. Cheng Z H, Gao L, Deng Z T, Jiang N, Liu Q, Shi D X, Du S X, Guo H M and Gao H J 2007 *J. Phys. Chem. C.* **111** 9240
30. Kalyuzhny G, Vaskevich A, Ashkenasy G, Shanzer A and Rubinstein I 2000 *J. Phys. Chem. B* **104** 8238
31. Lindsey J S and Wagner R W 1989 *J. Org. Chem.* **54** 828
32. Sivanesan A and John S A 2008 *Langmuir* **24** 2186
33. Tonezzer M, Quaranta A, Maggioni G, Carturan S and Della Mea G 2007 *Sens. Actuators B: Chem.* **122** 620

34. Chen H T, Liu B, Wang H T, Xiao Z D, Chen M and Qian D 2007 *J Mater. Sci. Eng. C* **27** 639
35. Knyukshto V N, Solovyov K N and Egorova G D 1998 *Biospectroscopy* **4** 121
36. Christian G D 2004 *Analytical chemistry*, sixth ed., Singapore: John Wiley & Sons
37. Sehlotho N and Nyokong T 2006 *Electrochim. Acta* **51** 4463
38. Sivanesan A and John S A 2009 *Electrochim. Acta* **54** 7458
39. Huethorst J A M S and Fokkink L G J 1995 *Langmuir* **11** 2237
40. Tse Y H, Janda P, Lam H, Zhang J, Pietro W J and Lever A B P 1997 *J. Porphyrins Phthalocyanines* **1** 3
41. Janda P, Kobayashi N, Auburn P R, Lam H, Leznoff C C and Lever A B P 1989 *Can. J. Chem.* **67** 1109
42. Vijaikanth V, Capon J F, Gloaguen F, Schollhammer P, Talarmin J 2005 *Electrochem. Commun.* **7** 427
43. Maree S and Nyokong T 2000 *J. Electroanal. Chem.* **492** 120
44. Mashazi P N, Ozoemena K I, Maree D M and Nyokong T 2006 *Electrochim. Acta* **51** 3489
45. Kalimuthu P and John S A 2009 *Electrochem. Commun.* **11** 367